

Structural, transport, and thermal properties of single crystalline type-VIII clathrate $\text{Ba}_8\text{Ga}_{16}\text{Sn}_{30}$

D. Huo,^{1,2} T. Sakata,² T. Sasakawa,² M. A. Avila,² M. Tsubota,²
F. Iga,² H. Fukuoka,³ S. Yamanaka,³ S. Aoyagi,⁴ and T. Takabatake²

¹College of Materials Science and Engineering, Donghua University, Shanghai 200051, China

²Department of Quantum Matter, ADSM, Hiroshima University, Higashi-Hiroshima 739-8530, Japan

³Department of Applied Chemistry, Hiroshima University, Higashi-Hiroshima 739-8527, Japan

⁴The Japan Synchrotron Radiation Research Institute, SPring-8, Hyogo 679-5108, Japan

We report the electrical resistivity ρ , Hall coefficient R_H , thermoelectric power S , specific heat C , and thermal conductivity κ on single crystals of the type-VIII clathrate $\text{Ba}_8\text{Ga}_{16}\text{Sn}_{30}$ grown from Sn-flux. Negative S and R_H over a wide temperature range indicate that electrons dominate electrical transport properties. Both $\rho(T)$ and $S(T)$ show typical behavior of a heavily doped semiconductor. The absolute value of S increases monotonically to 243 $\mu\text{V/K}$ with increasing temperature up to 550 K. The large S may originate from the low carrier concentration $n=3.7\times 10^{19} \text{ cm}^{-3}$. Hall mobility μ_H shows a maximum of 62 cm^2/Vs around 70 K. The analysis of temperature dependence of μ_H suggests a crossover of dominant scattering mechanism from ionized impurity to acoustic phonon scattering with increasing temperature. The existence of local vibration modes of Ba atoms in cages composed of Ga and Sn atoms is evidenced by analysis of experimental data of structural refinement and specific heat, which give an Einstein temperature of 50 K and a Debye temperature of 200 K. This local vibration of Ba atoms should be responsible for the low thermal conductivity (1.1 W/m K at 150 K). The potential of type-VIII clathrate compounds for thermoelectric application is discussed.

I. INTRODUCTION

Semiconducting clathrate compounds are attracting considerable attention because of their potential applications in thermoelectrics.¹ These compounds consist of face-shared polyhedral cages (formed by Si, Ge, Sn, and/or Ga) filled with alkali-metal, alkaline-earth and/or rare-earth atoms. The most pronounced feature of clathrate compounds is their very low lattice thermal conductivity κ_L ($\sim 1 \text{ W/m K}$ at room temperature). Some compounds even show glasslike temperature-dependent thermal conductivity, although they crystallize in well-defined structures. These classes of compound are good candidates to fulfill the phonon glass electron crystals (PGECs) concept,² which is a guideline to search for high performance thermoelectric materials with the compatibility of low thermal conductivity and high electrical conductivity. The thermoelectric performance of a material at a given operation temperature T is characterized by the dimensionless figure of merit ZT , which is defined as $ZT=S^2T/\rho(\kappa_L+\kappa_e)$, where S , ρ , κ_e are the thermoelectric power, electrical resistivity, and electronic thermal conductivity of the material, respectively. A higher energy conversion efficiency demands a large ZT . However, ZT has been limited to unity for several decades although much effort has been made to increase it.

Recently, within the spirit of PGEC concept, open structured compounds such as filled skutterudites and clathrates have been extensively investigated due to their low κ_L , which leads to a much-enhanced ZT .^{1,3,4} The reduction of thermal conductivity for these compounds is believed resultant from the local vibrations (rattling) of the guest atoms encapsulated in oversized cages. The heat-carrying phonons are scattered effectively by the

rattling of these guest atoms. However, the mechanisms responsible for some clathrate compounds showing glasslike $\kappa(T)$ at low temperatures remain an open issue. Based on the experimental results of neutron scattering and ultrasonic attenuation on single crystals of $X_8\text{Ga}_{16}\text{Ge}_{30}$ ($X = \text{Ba}, \text{Sr}, \text{Eu}$),^{5,6} it was concluded that the scattering of phonons from tunneling states is responsible for the glasslike $\kappa(T)$ of $(\text{Sr/Eu})_8\text{Ga}_{16}\text{Ge}_{30}$ in addition to the scattering from the rattling guest atoms. The absence of glasslike $\kappa(T)$ for the n -type $\text{Ba}_8\text{Ga}_{16}\text{Ge}_{30}$ sample was attributed to a very low density of tunneling states, if any. On the other hand, Bentien *et al.*⁷ recently reported a glasslike $\kappa(T)$ of a Ga-rich p -type $\text{Ba}_8\text{Ga}_{16}\text{Ge}_{30}$. They discussed the difference in thermal conductivity between the two types of samples and pointed out that glasslike $\kappa(T)$ of $(\text{Ba/Sr/Eu})_8\text{Ga}_{16}\text{Ge}_{30}$ at low temperatures ($< 15 \text{ K}$) is determined by scattering of phonons on charge carriers. Most recently, Bridges and Downward proposed another possible mechanism for the glasslike $\kappa(T)$ of clathrates.⁸ They argued that off-center displacement of guest atoms is crucial for understanding the glasslike behavior in $\kappa(T)$. Therefore, it is important to investigate the origin of the glasslike $\kappa(T)$ in clathrate compounds using single crystals to exclude effects of other factors, such as scattering at grain boundaries. The existence of large number of clathrate compounds and the amenability of their framework supply opportunities for us to bring the issue to a close, and to find high performance thermoelectric materials among them.

Until today, most of the work on clathrate compounds has been focusing on type-I clathrates of silicon,^{9,10} germanium,^{5,11,12} and tin.¹³ In this paper, we present a comprehensive study on single crystals of $\text{Ba}_8\text{Ga}_{16}\text{Sn}_{30}$,

which crystallizes in the type-VIII clathrate structure (SG: $cI54$).^{14,15} There are only two known members in this family of clathrates. The other is the α -phase of $\text{Eu}_8\text{Ga}_{16}\text{Ge}_{30}$, which transforms to β -phase (type-I clathrate) above 696 °C.^{5,11} One of the structural features for type-VIII clathrate compounds is that there is only one kind of polyhedral cage for the guest atoms, differing from the two kinds of cage in both type-I and type-II clathrates. In $\text{Ba}_8\text{Ga}_{16}\text{Sn}_{30}$, Ba atoms are encapsulated in cages composed of 23 atoms of $E = (\text{Ga}, \text{Sn})$, which are derived from pentagonal dodecahedra composed of E_{20} atoms. The existence of small E_8 voids in the network of E_{46} is another feature of type-VIII clathrates. We were motivated to investigate the title compound in detail by the few reports on it in literature with a scattering of lattice parameters, different melting behaviors, and promising thermoelectric properties. Recently, we succeeded in growing large single crystals of $\text{Ba}_8\text{Ga}_{16}\text{Sn}_{30}$. The structural, transport, and thermal properties are presented here.

II. EXPERIMENT

A. Crystal growth and structure refinement

Single crystals were grown from Sn-flux. High purity elements were mixed in an atomic ratio of $\text{Ba}:\text{Ga}:\text{Sn} = 8:16:60$ in an argon atmosphere glovebox. The mixture sealed in an evacuated and carbonized silica tube was heated slowly to 1270 K and reacted for 5 hours. Then, it was cooled to room temperature in two steps: fast cooled to 720 K at first and kept at this temperature for 12 hours, then slowly cooled down to room temperature. The well-shaped crystals of 10 mm in diameter with a shiny metallic luster were separated from the molten Sn solvent by centrifuging. The crystals are not sensitive to air and moisture. Polished surfaces of the crystals were examined by the use of optical microscopy and Laue x-ray reflection to confirm their homogeneous single-crystal nature. The composition of the crystals was examined by electron probe microanalysis (EPMA) with a JEOL JXA-8200 microanalyzer. The same result with a composition of $\text{Ba}_8\text{Ga}_{16.0}\text{Sn}_{30.7}$ was obtained on several crystals, which is nearly the ideal stoichiometric composition. Because Carrillo-Cabrera *et al.*¹⁵ suggested a positive thermoelectric power of a Ga-rich sample in a short report, we have tried to grow crystals in Ga-flux with initial atomic ratio of $\text{Ba}:\text{Ga}:\text{Sn} = 8:38:30$. However, we obtained the stoichiometric crystals again, so the stoichiometric compound seems to be very stable. The structure was refined with a Rigaku R-Axis diffractometer and with synchrotron radiation powder x-ray diffraction (XRD) from 100 to 390 K. The powder XRD experiment was carried out by using a large Debye-Scherrer camera installed at beam line BL02B2, SPring-8, Japan. The wavelength of the incident x-ray was 0.735 Å.

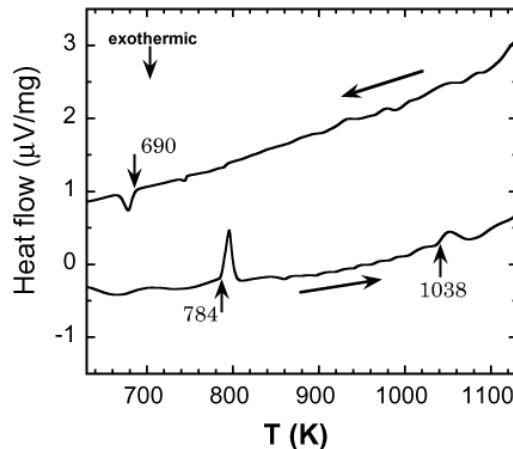


FIG. 1: Differential thermal analysis curves for $\text{Ba}_8\text{Ga}_{16}\text{Sn}_{30}$.

B. Measurements of thermal and transport properties

Differential thermal analysis (DTA) was performed from room temperature to 1200 K with ruthenium as a standard. The electrical resistivity (thermoelectric power) was measured with a homemade cryostat from 3 (5) to 300 K, and measured from 100 to 500 K (550 K) with a commercial MMR measurement system. The data obtained with the two systems are in good agreement in the overlapped temperature range. The Hall coefficient was measured under a magnetic field of 1 Tesla from 4 to 300 K. Thermal conductivity was measured with a steady-state method from 1.5 to 150 K with a homemade cryostat. The measurements of specific heat were carried out from 2 to 300 K with a PPMS (Quantum Design).

III. RESULTS AND DISCUSSION

It was reported at first that $\text{Ba}_8\text{Ga}_{16}\text{Sn}_{30}$ melts congruently at 723 K,¹⁴ whereas, Kuznetsov *et al.*¹⁶ observed an incongruent melting behavior with a decomposition temperature of 740 K and liquidus temperature of 784 K. In order to check which is the case, a DTA measurement was carried out on our small single crystals. Figure 1 shows the heating and cooling DTA curves. The double peaks on the heating curve indicate an incongruent melting nature of this compound. However, we observed a decomposition temperature of 784 K and liquidus temperature of 1038 K, which are higher than those reported in Ref.16. This information helped us to succeed in growing large single crystals of $\text{Ba}_8\text{Ga}_{16}\text{Sn}_{30}$ by cooling down the reactant in two steps as described above.

The single-crystal XRD data were collected at 293, 253 and 123 K, respectively. The cubic crystal structure of type-VIII clathrate for $\text{Ba}_8\text{Ga}_{16}\text{Sn}_{30}$ was confirmed. The lattice parameter decreases from 11.586(1) to 11.5831(4)

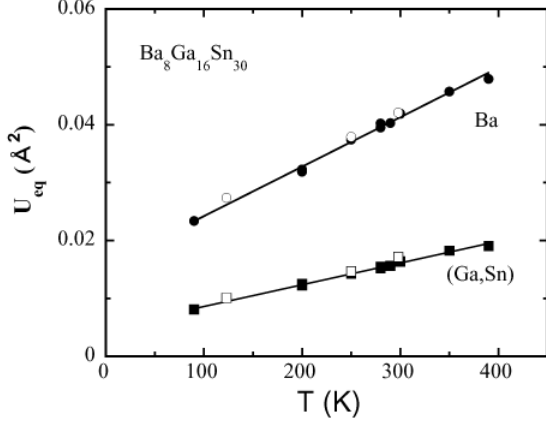


FIG. 2: Temperature dependence of isotropic atomic displacement parameters U_{eq} of $\text{Ba}_8\text{Ga}_{16}\text{Sn}_{30}$. Open symbols: data determined by structural refinement from single crystal XRD. Closed symbols: data determined by structural refinement from synchrotron radiation powder XRD.

to 11.5619(3) Å with decreasing temperature correspondingly. The structural refinement gives a composition of $\text{Ba}_8\text{Ga}_{16.2}\text{Sn}_{29.8}$, which is in good agreement with the results of EPMA. The high resolution powder XRD analysis using synchrotron radiation gives consistent results also. With decreasing temperature from 390 to 100 K, there is a normal thermal contraction, but no change in structure was observed. There is no indication of split sites for Ba atoms down to 100 K.

Here, we pay attention to the atomic displacement parameters (ADPs) obtained from XRD analysis. As a first approximation, the guest atoms in clathrate compounds may be treated as Einstein oscillators, which vibrate independently with the same frequency, and the framework atoms as a Debye solid. It has been proved to be successful in giving a reasonable estimation of the Einstein temperature Θ_E , Debye temperature Θ_D and room-temperature thermal conductivity with ADPs of the guest and framework atoms.¹⁷ Figure 2 shows the temperature dependences of the isotropic ADPs for $\text{Ba}_8\text{Ga}_{16}\text{Sn}_{30}$. The open and closed symbols denote the results from single-crystal XRD analysis and synchrotron radiation powder XRD analysis, respectively, which are in good agreement. The ADPs of Ba atoms are much larger than those of framework atoms (Ga,Sn), which indicates the rattling of Ba atoms in the oversized cages as in the $\text{Ba}_8\text{Ga}_{16}\text{Ge}_{30}$.⁵ The two straight lines, which do not pass through the origin by extrapolation, are linear fits of the data. Using the slopes of these straight lines, $U_{eq}/T = h^2/(4\pi^2 m_r k_B \Theta_E^2)$ and $U_{eq}/T = 3h^2/(4\pi^2 m_{av} k_B \Theta_D^2)$ (where m_r and m_{av} are mass of the rattler atom and average mass of the framework atoms, respectively), $\Theta_E = 64$ K and $\Theta_D = 195$ K for $\text{Ba}_8\text{Ga}_{16}\text{Sn}_{30}$ were obtained. As discussed below, they are close to the two characteristic temperatures extracted from specific heat data. Because there are no

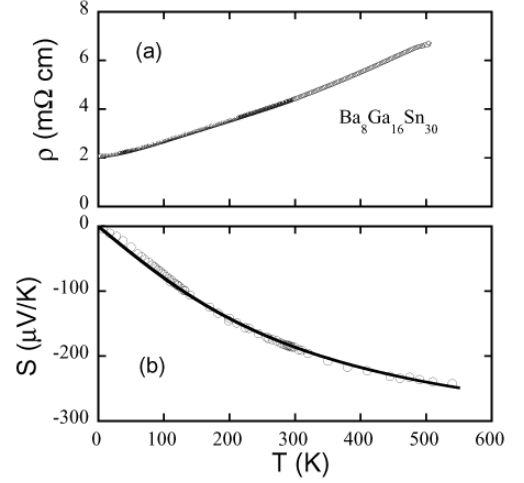


FIG. 3: (a) Temperature dependence of electrical resistivity ρ and (b) thermoelectric power S of $\text{Ba}_8\text{Ga}_{16}\text{Sn}_{30}$. The solid line is a calculation result (see text).

evident split sites in $\text{Ba}_8\text{Ga}_{16}\text{Sn}_{30}$ from XRD analysis, the Ba atoms in this compound are normal rattlers like in $\text{Ba}_8\text{Ga}_{16}\text{Ge}_{30}$. The large ADP values describe rattling of Ba atoms around the centers of their crystallographic sites.

The temperature dependence of the electrical resistivity ρ and thermoelectric S of $\text{Ba}_8\text{Ga}_{16}\text{Sn}_{30}$ is shown in Fig. 3. On cooling, $\rho(T)$ decreases monotonically from 6.6 mΩ cm (500 K) to 2.0 mΩ cm (3 K), being typical of heavily doped semiconductors. Our observation is contrasting with the results in Ref.16, where a typical semiconductor behavior with a value of 15 meV for activation energy was observed. The carrier concentration n ($2.2 \times 10^{19} \text{ cm}^{-3}$) of their polycrystalline sample at room temperature is a little smaller than that of our single-crystal sample $n(300 \text{ K}) = 3.7 \times 10^{19} \text{ cm}^{-3}$ (see below). This difference might be responsible for the different behavior in $\rho(T)$. Metal-like temperature dependence of ρ was reported for a Ga-rich polycrystalline sample.¹⁵

The absolute value of S increases monotonically with increasing temperature up to 550 K. The overall features of the $S(T)$ resemble the previously reported results in Ref.16. However, the maximum at about 500 K reported in Ref.16 does not exist in our data in Fig. 3(b). The discrepancy might result from the possibility that our accessible temperature was not high enough to observe a maximum or from distinct quality between our single-crystal sample and their polycrystalline sample.

As the detailed energy band structure of $\text{Ba}_8\text{Ga}_{16}\text{Sn}_{30}$ is not known yet, the $S(T)$ and band effective mass m^* are evaluated by an assumption of one parabolic conduction band model with different scattering mechanisms. The overall feature of $S(T)$ could be reproduced well by a single-band model with dominant ionized impurity scattering. In this model the thermoelectric power and the

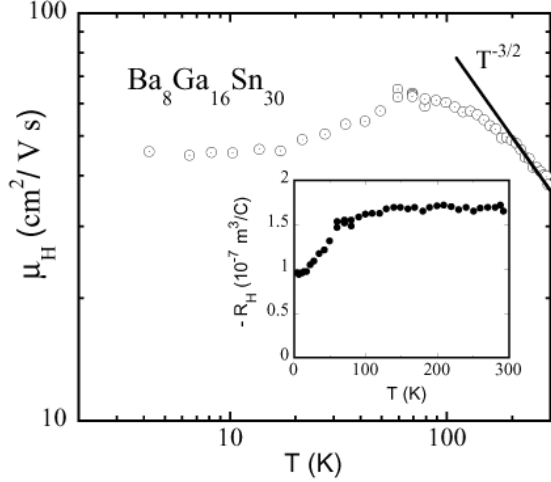


FIG. 4: Temperature dependence of Hall mobility μ_H of $\text{Ba}_8\text{Ga}_{16}\text{Sn}_{30}$. Inset shows temperature dependence of Hall coefficient R_H of $\text{Ba}_8\text{Ga}_{16}\text{Sn}_{30}$.

carrier concentration is given by¹⁸

$$S(T) = \frac{k_B}{e} \left(\frac{4F_3(\eta)}{3F_2(\eta)} - \eta \right) \quad (1)$$

$$n = \frac{(2m^*k_B T)^{3/2}}{2\pi^2\hbar^3} F_{1/2}(\eta) \quad (2)$$

where F_x is Fermi-Dirac integral of the order x , η is reduced Fermi energy defined as $\eta = E_F/k_B T$ (E_F is Fermi energy).

The solid line in Fig. 3(b) is the calculated $S(T)$ with $E_F = 88$ meV, which reproduces our experimental data very well. The estimated band effective mass $m^* = 0.14m_0$ (m_0 is the free electron mass) was obtained by using the Fermi energy and the room temperature carrier concentration. The m^* value is one order of magnitude smaller than $3.6m_0$ for the type-I clathrate $\text{Ba}_8\text{Ga}_{16}\text{Ge}_{30}$ estimated by the similar method.⁷ Recently, band structure calculation was reported for Eu filled type-VIII clathrate of germanium, which suggests that the low band effective mass might be inherent to n -doped type-VIII clathrates due to their structural features.¹⁹ The disperse bands centered around the E_8 voids in VIII clathrates would be responsible for the low m^* . However, there is not enough experimental data to examine whether it is inherent or not because the member of type-VIII clathrates is limited to 2 at present.

In order to get further insights into the carrier scattering mechanisms in $\text{Ba}_8\text{Ga}_{16}\text{Sn}_{30}$, the Hall coefficient R_H was measured from 4 to 300 K. As shown in Fig. 4, R_H is negative in the overall temperature range. The negative S and R_H over a wide temperature range indicate the majority carriers being electrons in $\text{Ba}_8\text{Ga}_{16}\text{Sn}_{30}$. Assuming a one band model, the carrier concentration n (=

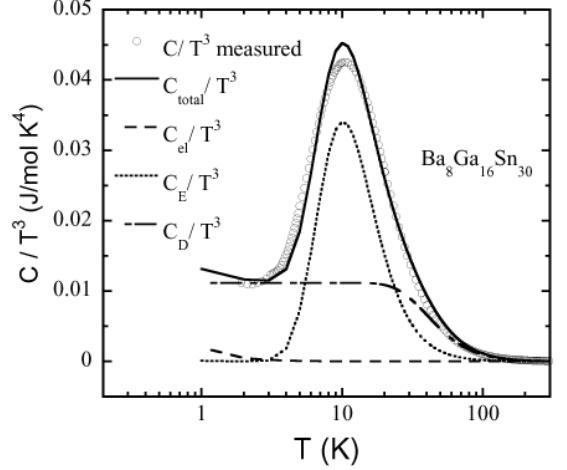


FIG. 5: Temperature dependence of specific heat C of $\text{Ba}_8\text{Ga}_{16}\text{Sn}_{30}$. The lines are results of fitting (see text).

$1/eR_H$) is derived to be $3.7 \times 10^{19} \text{cm}^{-3}$ at 300 K, which is increased to $6.6 \times 10^{19} \text{cm}^{-3}$ at 4 K. The Hall mobility $\mu_H = |R_H|/\rho$ is plotted in the inset of Fig. 4 as a function of temperature. At room temperature, $\mu_H = 39 \text{ cm}^2/\text{V s}$, is larger than $20 \text{ cm}^2/\text{V s}$ of $\alpha\text{-Eu}_8\text{Ga}_{16}\text{Ge}_{30}$ (Ref. 11) and $26 \text{ cm}^2/\text{V s}$ of a $\text{Ba}_8\text{Ga}_{16}\text{Sn}_{30}$ polycrystalline sample.¹⁶ In the relaxation time approximation, temperature dependence of $\mu_H \propto T^\alpha$ determines the carrier scattering mechanism: μ_H taking the values of $3/2$, 0 , $-3/2$ for ionized impurity, neutral impurity, and acoustic phonon scattering, respectively.²⁰ However, it is difficult to observe the ideal power law of μ_H experimentally over a wide temperature range in a real solid. Instead, a mixed scattering process of ion impurity and acoustic phonon scattering is usually observed.²¹ For the present compound, μ_H shows weak temperature dependence below 20 K, increases with increasing temperature between 20 and 70 K, then decreases above 80 K. An approximately $T^{-3/2}$ dependence was observed near 300 K. This temperature dependence of μ_H indicates a crossover from dominant charge carrier scattering by neutral impurities below 20 K to acoustic phonon scattering at higher temperature via an ionized impurity scattering range.

As mentioned earlier, in first approximation, the Ba atoms could be considered as Einstein oscillators and the framework composed of $(\text{Ga}, \text{Sn})_{46}$ clusters as a Debye solid. Following this approach, the specific heat of $\text{Ba}_8\text{Ga}_{16}\text{Sn}_{30}$ is treated as a sum of three terms: an electronic contribution C_{el} , a Debye contribution C_D , and an Einstein contribution C_E with Θ_E of the order of several tens Kelvin. The low-energy vibrating modes would greatly contribute to low-temperature specific heat. To elucidate the evidence for the low-energy modes in $\text{Ba}_8\text{Ga}_{16}\text{Sn}_{30}$, the specific heat was measured from 2 to 300 K. In order to emphasize the contribution of the local modes, the data are shown in Fig. 5 as a plot of C/T^3 vs T . It can be seen clearly that a broad peak

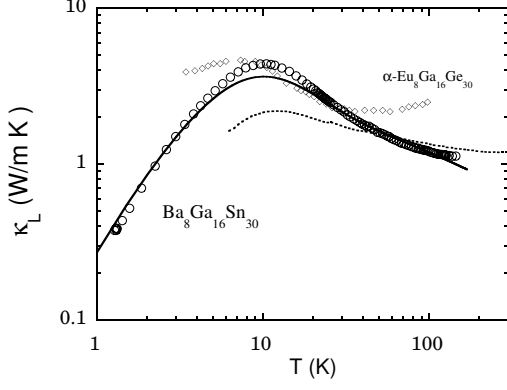


FIG. 6: Temperature dependence of lattice thermal conductivity κ_L of $\text{Ba}_8\text{Ga}_{16}\text{Sn}_{30}$. The solid line is a fit of data (see text). The data of κ_L for $\alpha\text{-Eu}_8\text{Ga}_{16}\text{Ge}_{30}$ (\diamond) and a polycrystalline sample of $\text{Ba}_8\text{Ga}_{16}\text{Sn}_{30}$ (dashed line) were taken from Ref. 11 and Ref. 23, respectively.

centered at 10 K exists. In the C/T^3 vs T plot, the Debye contribution approaches a constant at low temperatures. For semiconducting clathrate compounds, the electronic contribution to specific heat is a small portion of the total specific heat at low temperatures and becomes relatively smaller with increasing temperature. Therefore, the peak mainly comes from the local vibrating modes. With this analysis, we fit the data to an expression of specific heat $C/T^3 = \gamma/T^2 + N_E C_E/T^3 + N_D C_D/T^3$. With the electronic specific heat coefficient γ of 1.3 mJ/molK² obtained from the low-temperature plot of $C(T)/T$ vs T^2 , we further fixed the numbers of Debye and Einstein oscillators to $N_E = 8$ and $N_D = 46$, respectively, which are the numbers of guest Ba atoms and framework atoms of (Ga,Sn) per formula unit. Then the fitting parameters are just the two characteristic temperatures Θ_D and Θ_E . The fitting results for the three contributions and their sum C_{total} are shown together in Fig. 5. The two parameters obtained from the fitting are $\Theta_D = 200$ K and $\Theta_E = 50$ K. They are close to the values of 195 K and 64 K estimated with ADPs. Considering the simplicity of the model, the fit with two parameters is fairly good. Better agreement could be achieved by assuming a distribution of Θ_E like the approach in the analysis of specific heat data of ZrW_2O_8 .²² Furthermore, coupling effects between the local modes of guest atoms and low-frequency acoustic phonons of the framework atoms should be taken into account.

It is believed that the scattering of heat-carrying acoustic phonons of the framework atoms by the local modes of the guest atoms is responsible for the reduction of thermal conductivity. The lattice thermal conductivity κ_L of $\text{Ba}_8\text{Ga}_{16}\text{Sn}_{30}$ is plotted as a function of temperature in Fig. 6. For comparison, previously reported data of $\kappa_L(T)$ are also shown for polycrystals of $\text{Ba}_8\text{Ga}_{16}\text{Sn}_{30}$ (Ref. 23) and $\alpha\text{-Eu}_8\text{Ga}_{16}\text{Ge}_{30}$ (Ref. 11). At low temper-

atures, the $\kappa_L(T)$ of our single crystal is larger than that of the polycrystalline sample,²³ in which scattering of phonons at grain boundaries might greatly contribute to the reduction of $\kappa_L(T)$. The $\kappa_L(T)$ of the two type-VIII clathrate compounds is characterized by a peak at about 10 K. A significant peak in $\kappa_L(T)$ is typical of a crystalline solid, differing from the glasslike $\kappa_L(T)$ observed for $(\text{Sr}/\text{Eu})_8\text{Ga}_{16}\text{Ge}_{30}$ type-I clathrates.⁵ Below the temperature of the peak, κ_L of $\text{Ba}_8\text{Ga}_{16}\text{Sn}_{30}$ decreases faster than that of $\alpha\text{-Eu}_8\text{Ga}_{16}\text{Ge}_{30}$ with decreasing temperature.

A qualitative understanding of the contributions from different scattering mechanisms to κ_L could be reached by analysis of $\kappa_L(T)$ data with a phenomenological model.^{11,24,25} In this model, the lattice thermal conductivity is formulated as following:

$$\kappa_L = \frac{\nu}{3} \int_0^{\omega_D} C(\omega) l(\omega) d\omega \quad (3)$$

with $l = (l_{TS}^{-1} + l_{Res}^{-1} + l_R^{-1})^{-1} + l_{min}$, $l_{TS}^{-1} = A(\hbar\omega/k_B) \tanh(\hbar\omega/2k_B T) + (A/2)(k_B/\hbar\omega + B^{-1}T^{-3})^{-1}$, $l_{Res}^{-1} = \sum C_i \omega^2 T^2 / [(\omega_i^2 - \omega^2)^2 - \gamma_i(\omega_i \omega)^2]$, and $l_R^{-1} = D(\hbar\omega/k_B)^4$, where ν is the average velocity of sound, $C(\omega)$ is the Debye specific heat, and $l(\omega)$ is the total mean free path of phonons with frequency of ω . The three components of $l(\omega)$ correspond to the contributions from different scattering mechanisms: tunneling states (l_{TS}), Rayleigh scattering (l_R), and resonant scattering (l_{Res}). The lower limit of $l(\omega)$ is constrained to a constant l_{min} . We followed the approach in Ref. 11 to reduce the number of fitting parameters. Two parameters, i.e., the velocity of sound $\nu = (\Theta_D k_B / \hbar) / (6\pi^2 n_A)^{1/3}$ (n_A is the number of atoms per unit volume) and resonant frequency $\omega_E = k_B \Theta_E / \hbar$ were fixed, respectively, by use of the Debye temperature $\Theta_D = 200$ K and Einstein temperature $\Theta_E = 50$ K obtained from the experiments of specific heat. Other parameters (A, B, C, D, γ_1) were obtained by fitting the data to the model. The solid line in Fig. 6 shows a fit with a set of reasonable parameters: $A = 1.08 \times 10^4 \text{ m}^{-1} \text{K}^{-1}$, $B = 5.0 \times 10^{-1} \text{K}^{-2}$, $C = 1.0 \times 10^{30} \text{ m}^{-1} \text{s}^{-2} \text{K}^{-2}$, $D = 2.6 \text{ m}^{-1} \text{K}^{-4}$, $\gamma_1 = 0.8$. The ratio of A/B is a measure of the density of tunneling states per unit volume strongly coupled to phonons.²⁴ Here, we obtained $A/B = 2.2 \times 10^4 \text{ m}^{-1} \text{K}^{-3}$. This ratio is comparable to $3.7 \times 10^4 \text{ m}^{-1} \text{K}^{-3}$ of $\alpha\text{-Eu}_8\text{Ga}_{16}\text{Ge}_{30}$ (type-VIII), but much smaller than $3.6 \times 10^6 \text{ m}^{-1} \text{K}^{-3}$ for $\beta\text{-Eu}_8\text{Ga}_{16}\text{Ge}_{30}$ (type-I), which shows glasslike $\kappa_L(T)$.¹¹ It is suggestive that the density of tunneling states is very low in the type-VIII clathrates if any. It is straightforward to understand if one attribute the glasslike $\kappa_L(T)$ to the tunneling of guest atoms among the split sites, which are absent in type-VIII clathrates. Massive and smaller guest atom, such as Eu and Sr, filled type-VIII clathrate of tin is expected to show glasslike thermal conductivity because Eu/Sr atoms would have split sites or have much more room to move around in cages if off-center displacement of guest atoms is really responsible for glasslike thermal conductivity as suggested in Ref. 8.

The stability of Sr filled type-VIII clathrate $\text{Sr}_8\text{Ga}_{16}\text{Ge}_{30}$ is predicted from band calculation,¹⁹ but has not been confirmed experimentally.

A dimensionless figure of merit $ZT = 0.15$ at 300 K for $\text{Ba}_8\text{Ga}_{16}\text{Sn}_{30}$ is estimated from the present set of data. For thermoelectric application, the ZT should be improved by optimal doping level and further reduction of thermal conductivity. As mentioned above, a massive and smaller guest atom, such as Eu, filled type-VIII clathrate is expected to have lower thermal conductivity. Furthermore, band structure calculation on type-VIII Ge-clathrate suggests that p -doped type-VIII clathrate is promising for thermoelectric application, for which a figure of merit of 1.2 at 400 K is predicted. Therefore, it is interesting to fabricate and study p -doped type-VIII clathrate compounds.

IV. SUMMARY

Single crystals of type-VIII clathrate compound $\text{Ba}_8\text{Ga}_{16}\text{Sn}_{30}$ were grown from Sn-flux. Incongruent melting nature of this compound was confirmed by differential thermal analysis. Negative thermoelectric power and Hall coefficient indicate electrons dominating the transport properties. The estimated band effective mass $0.14m_0$ is smaller than that of type-I clathrate compounds. The large absolute value of thermoelectric power (188 $\mu\text{V}/\text{K}$ at 300 K) may originate from the low carrier

concentration $n(300\text{ K}) = 3.7 \times 10^{19}\text{ cm}^{-3}$. Hall mobility μ_H shows a maximum of 62 $\text{cm}^2/\text{V s}$ around 70 K. The analysis of the temperature dependence of μ_H suggests a crossover of dominant scattering mechanism from ion impurity at low temperatures to acoustic phonon scattering at high temperatures. Although the $\kappa(T)$ shows a pronounced peak, being typical of crystalline solids, the value of thermal conductivity is reduced very much. $\kappa = 1.1\text{ W/m K}$ at 150 K. The reduction in $\kappa(T)$ is attributed to the rattling of Ba atoms in the cages composed of Ga and Sn atoms. The evidence of this rattling is elucidated by the analysis of experimental data of XRD and specific heat, which gives the estimation of $\Theta_D = 200$ and $\Theta_E = 50\text{ K}$, respectively. It is interesting to study p -doped type-VIII clathrate compounds to examine the predictions of band structure calculations that these compounds should have prospective thermoelectric properties.

D.H. acknowledges the financial support from JSPS. We thank Y. Shibata for the electron-probe microanalysis. This work was supported by a Grant-in Aid for Scientific Research (COE 13CE2002) and a Grant-in-Aid for Scientific Research in Priority Area "Skutterudite" (No.15072205) of MEXT Japan. The synchrotron x-ray diffraction was performed at the BL02B2 in SPring-8 under Proposal No. 2003A0247.

-
- ¹ G. S. Nolas, in *Semiconductors and semimetals*, vol.69, edited by T.M. Tritt, (Academic Press, San Diego, 2001) p.255.
 - ² G. A. Slack, in *CRC Handbook of Thermoelectrics*, edited by D.M. Rowe (CRC Boca Raton, 1995), p. 407.
 - ³ C. Uher, in *Semiconductors and semimetals*, vol.69, edited by T.M. Tritt, (Academic Press, San Diego, 2001) p.139.
 - ⁴ G. S. Nolas, J. L. Cohn, G. A. Slack, and S. B. Schujman, *J. Appl. Phys.* **73**,178 (1998).
 - ⁵ B. C. Sales, B.C. Chakoumakos, R. Jin, J.R. Thompson, and D. Mandrus, *Phys. Rev. B* **63**, 245113 (2001).
 - ⁶ V. Keppens, B. C. Sales, D. Mandrus, B. C. Chakoumakos, C. Laermans, *Philos. Mag. Lett.* **80**, 807 (2000).
 - ⁷ A. Bentien, M. Christensen, J. D. Bryan, A. Sanchez, S. Paschen, F. Steglich, G. D. Stucky, and B.B. Iversen, *Phys. Rev. B* **69**, 45107 (2004).
 - ⁸ F. Bridges and L. Downard, arXiv:com-mat/0311250.
 - ⁹ H. Fukuoka, J. Kiyoto, S. Yamanaka, *Inorg. Chem.* **42**, 2933 (2003).
 - ¹⁰ M. Imai, K. Nishida, T. Kimura, K. Yamada, *J. Alloys Comp.* **335**, 270 (2002).
 - ¹¹ S. Paschen, W. Carrillo-Cabrera, A. Bentien, V. H. Tran, M. Baenitz, Y. Grin, and F. Steglich, *Phys. Rev. B* **64**, 214404 (2001).
 - ¹² J. Dong, and O.F. Sankey, *J. Phys. Condens. Matter* **11**, 6129 (1999).
 - ¹³ G. S. Nolas, J. L. Cohn, J. S. Dyck, C. Uher, and J. Yang, *Phys. Rev. B* **65**, 165201 (2002).
 - ¹⁴ B. Eisenmann, H. Schafer, and R. Zahler, *J. Less-Common Metals* **118**, 43 (1986).
 - ¹⁵ W. Carrillo-Cabrea, R. C. Gil, V. H. Tran, and Y. Grin, *Z. Kristallorg. NCS* **217**, 181 (2002).
 - ¹⁶ V. L. Kuznetsov, L. A. Kuzentsova, A. E. Kaliazin, and D. M. Rowe, *J. Appl. Phys.* **87**, 7871 (2000).
 - ¹⁷ B. C. Sales, B. C. Chakoumakos, D. Mandrus, and J. W. Sharp, *J. Solid State Chem.* **146**, 528 (1999).
 - ¹⁸ D. R. Lovett, *Semimetals & Narrow-Bandgap Semiconductors* (Pion Limited, London, 1977).
 - ¹⁹ G. K.H. Madsen, K. Schwarz, P. Blaha, and D. J. Singh, *Phys. Rev. B* **68**, 125212 (2003).
 - ²⁰ K. Seeger, *Semiconductor physics: an introduction* (Springer-Verlag, 1985).
 - ²¹ J. S. Dyck, W. Chen, C. Uher, L. D. Chen, X. F. Tang, and T. Hirai, *J. Appl. Phys.* **91**, 3698 (2002).
 - ²² A. P. Ramirez and G.R. Kowach, *Phys. Rev. Lett.* **80**, 4903 (1998).
 - ²³ G. S. Nolas, *Mat. Res. Soc. Symp. Pro.* **545**, 435 (1999).
 - ²⁴ J. L. Cohn, G. S. Nolas, V. Fessatidis, T. H. Metcalf, and G. A. Slack, *Phys. Rev. Lett.* **82**, 779 (1999).
 - ²⁵ G. S. Nolas, T. J. R. Weakley, J. L. Cohn, and R. Sharma, *Phys. Rev. B* **61**, 3845 (2000).